International Journal of Biological Macromolecules 251 (2023) 126276

Contents lists available at ScienceDirect

International Journal of Biological Macromolecules

journal homepage: www.elsevier.com/locate/ijbiomac

Acylhydrazone-derived whole pectin-based hydrogel as an injectable drug delivery system

Shu-ya Wang [a,b,1], Maryamgul Tohti [a,1], Jia-qi Zhang [a], Jun Li [a], De-qiang Li [a,*]

[a] Xinjiang Key Laboratory of Agricultural Chemistry and Biomaterials, College of Chemistry and Chemical Engineering, Xinjiang Agricultural University, Urumchi 830052, Xinjiang, People's Republic of China
[b] School of Bioengineering, Dalian University of Technology, Dalian 116024, Liaoning, People's Republic of China

ARTICLE INFO

Keywords:
Injectable hydrogel
Pectin
Acylhydrazone linkage
Self-healing
Drug delivery system

ABSTRACT

Injectable hydrogel-based drug delivery systems have attracted more and more attention due to their sustained-release performance, biocompatibility, and 3D network. The present study showed whole pectin-based hydrogel as an injectable drug delivery system, which was developed from oxidized pectin (OP) and diacylhydrazine adipate-functionalized pectin (Pec-ADH) via acylhydrazone linkage. The as-prepared hydrogels were characterized by ^{1}H NMR, FT-IR, and SEM techniques. The equilibrium swelling ratio of obtained hydrogel (i.e., sample gel 5) was up to 4306.65 % in the distilled water, which was higher than that in PBS with different pH values. Increasing the pH of the swelling media, the swelling ratio of all hydrogels decreased significantly. The results that involved the swelling properties indicated the salt- and pH-responsiveness of the as-prepared hydrogels. The drug release study presented that 5-FU can be persistently released for more than 12 h without sudden release. Moreover, the whole pectin-based hydrogel presented high cytocompatibility toward L929 cell lines, and the drug delivery system showed a high inhibitory effect on MCF-7 cell lines. All these results manifested that the acylhydrazone-derived whole pectin-based hydrogel was an excellent candidate for injectable drug delivery systems.

1. Introduction

Injectable hydrogel-based drug delivery systems can not only delay the release of loaded drugs from the matrix but also possess excellent biocompatibility and three-dimensional (3D) network structures with high water content similar to the extracellular matrix, which provides the possibility for clinical application [1,2]. Moreover, the local injection of hydrogel-based drug delivery systems enables the drug to reach the nidus directly and achieve the effect of localized drug release, consequently reducing the toxic and side effects of the drug to the body and the cost of disease treatment [3]. All these advantages ensure the potential of injectable hydrogel-based drug delivery systems in biomedical fields.

The hydrogel will be impaired by daily activities after injecting into the human body, thereby losing strength and metabolizing rapidly [4,5]. Improving the crosslinking density is a traditional strategy for enhancing mechanical strength but can reduce the porosity of hydrogels, decrease drug loading efficiency, and inhibit cell growth and tissue regeneration [6,7]. Thus, this method is unsuitable for injectable hydrogels, which will also extend the degradation time of hydrogels in vivo and the risk to the body; More importantly, the enhancement of mechanical strength goes against the syringeability [6,8–10]. To equilibrate the injectability and mechanical strength, self-healing strategies have been introduced to prepare injectable hydrogels.

Small molecules and natural macromolecules that can form non-covalent interactions (e.g., hydrophilic and hydrophobic interactions, hydrogen bonding, and Van der Waals forces) have been employed to fabricate self-healing injectable hydrogels for drug delivery [10]. For small molecules, the mechanical strength of the resultant injectable hydrogel is hard to be controlled due to the weak characteristic of non-covalent interactions [5]. Oppositely, natural macromolecules can be facilely formed biocompatible and biodegradable hydrogel with stronger mechanical properties, such as cellulose, chitosan, and pectin [8,11–14]. Thereinto, pectin is composed of α-(1 → 4)-D-linked galacturonic acids dominantly with advantages in probiotic, hypoglycemic, hypocholesterolemia, anti-cancer, and anti-inflammatory effects that

* Corresponding author.
E-mail addresses: lsx20131120a@163.com, ldq@xjau.edu.cn (D.-q. Li).
[1] The authors contributed equally to the present work.

https://doi.org/10.1016/j.ijbiomac.2023.126276
Received 28 January 2023; Received in revised form 19 July 2023; Accepted 9 August 2023
Available online 13 August 2023

Table 1
Proportion of feedstocks for preparation of hydrogel.

Feedstocks	Samples				
	Gel 1	Gel 2	Gel 3	Gel 4	Gel 5
Pec-ADH	0.06	0.06	0.14	0.1	0.06
OP3	0.14	–	–	–	–
OP4	–	0.14	–	–	–
OP5	–	–	0.06	0.1	0.14

other common polysaccharides do not possess [15]. Moreover, the heteropolysaccharides structure of pectin ensures its low crystallinity [9,11,16] compared with linear polysaccharides (e.g., cellulose and chitosan), consequently contributing to proper mechanical strength and high syringeability. Thus, pectin is the first-class feedstock for forming an injectable hydrogel.

Composite hydrogels with syringeability were prepared based on the physical interactions between soluble pectin chains and chitosan nanogels, which possessed poor mechanical strength [9]. We developed Diels-Alder crosslinked pectin/chitosan hybrid hydrogel with acceptable mechanical strength but poor injectability [11]. These phenomena were mainly affected by the following facts: (1) the cyclic glycosyls limited the rotation of C—C and C—O linkages, resulting in a high rigidity of the skeleton; (2) the irreversible chemical linkage and crystallization behavior of chitosan. Thus, a dynamic covalent bond-derived pectin-based hydrogel may achieve the balance between mechanical strength and syringeability. The abundant hydroxyl and carboxyl groups in the pectin molecules guaranteed the accessibility of chemical reactions including esterification, etherification, coupling, grafting, oxidation, and amidation reactions [15,16]. Periodate oxidation could cleavage the C2-C3 linkages in the d-galacturonic acid units and endow oxidized pectin (OP) with better flexibility which contributed to the syringeability. An et al. have obtained injectable hydrogels from OP and acylhydrazide functionalized poly(N-isopropylacrylamide-*stat*-acylhydrazide) via the acylhydrazone linkage [17]. The self-healing and injectable properties were excellent based on the flexible OP molecules. However, the potential toxicity of synthetic polymers has been criticized. Thus, the synthesis of whole natural macromolecules-based injectable hydrogels from OP will be excited.

The objective of the present study was to prepare pectin-based injectable hydrogel with self-healing and injectable properties. Hydrogels were from OP and adipodihydrazide-functionalized pectin (Pec-ADH) via the dynamic covalent acylhydrazone linkage. ^{1}H NMR, FT-IR, and SEM techniques were used to characterize the chemical structure and morphology of the obtained hydrogel. The injectability and self-healing performance of hydrogels were studied to explore their potential as injectable hydrogels. We also determined the swelling behavior of the as-prepared hydrogels under simulated physiological conditions to show their stability and stimulus responsiveness. 5-fluorouracil (5-FU) was in situ loaded into the hydrogel, and the release performances were calculated. Moreover, biocompatibility and inhibition of cancer cells were also determined. Compared with the published data, the present pectin-based hydrogels showed excellent self-healing and injectable performance with better cytocompatibility. All the results obtained in the present work showed the excellent potential of the acylhydrazone-derived whole pectin-based hydrogel as an injectable drug delivery system.

2. Experiment

2.1. Material

Low methoxyl citrus pectin (degree of esterification =27.3 %, Mw ~30,000 g/mol, and content of galacturonic acid ≥ 74 %) was obtained from Shanghai Macklin Biochemical Co., Ltd. (Shanghai, China). $NaIO_4$ was obtained from Sinopharm Group Chemical Reagent Co., Ltd. (Shanghai, China). Adipodihydrazide, 1-ethyl-3-(3-dimethyllaminopropyl) carbodiimide hydrochloride (EDC), and 1-hydroxypyrrolidin-2, 5-dione (NHS) were acquired from Bidepharm Co., Ltd. (Shanghai, China). All the chemicals were used without any pretreatment.

2.2. Preparation of oxidized pectin

The preparation of OP was performed on the published data with few modifications [12,18]. Ten grams of pectin were dispersed in 375 mL of aqueous ethanol with a ratio of 1:4 (ethanol/distilled water, v/v) and stirred for 24 h to dissolve the pectin completely. Different dosage of $NaIO_4$ (3, 4, and 5 g) was dissolved in 50 mL of distilled water and stirred for 15 min under dark conditions. Then $NaIO_4$ solution was added to the above-mentioned pectin solution and stirred for 2 h in the dark. Finally, excess ethylene glycol was added to the reaction system to terminate the oxidization. The solution was centrifuged and dialyzed for 3 d, followed by freeze drying to obtain the final products. The obtained oxidized pectin (OP) was noted as OP3, OP4, and OP5 according to the different dosages of $NaIO_4$. OP3, OP4, and OP5 have oxidization degrees of 30.31 %, 33.56 %, and 39.42 %, which were determined by potentiometric titration of hydroxylamine hydrochloride [19].

2.3. Preparation of acylhydrazine-functionalized pectin (Pec-ADH)

This process was similar to the preparation of amide in our previous report [11]. Pectin (2 g) was dissolved in 100 mL of distilled water. Then EDC/NHS partners with a mole:mole ratio of 1:1.1 were added to activate the carboxyl groups in pectin molecules and stirred for another 1 h at 25 °C. Finally, 15.66 g adipodihydrazide was added to the solution and stirred for 48 h at room temperature. The mixture was poured into a dialysis bag with an MWCO 3500 Da for 3 days and freeze-dried to obtain the product.

2.4. Preparation of hydrogel via acylhydrazone linkage

The preparation of hydrogel via acylhydrazone linkage was a typical Schiff base reaction. Pec-ADH and OP were dissolved in 2.5 mL of distilled water in cylindrical molds, respectively. The dosage of Pec-ADH and OP used for different gels were listed in Table 1. Then the OP solution and Pec-ADH solution were mixed and stirred for 5 min at room temperature to obtain the hydrogels (Gels 1–5), and the reaction illustration is shown in Fig. 1.

2.5. Characterization

The FT-IR spectroscopy of pectin, oxidized pectin, Pec-ADH, and hydrogel were determined by Fourier Transformed Infrared Spectrometer (Nicolet is5, Thermo Fisher Scientific, U.S.A). The microsamples were ground with 40 mg KBr, pressed into sheets, and scanned in the 4000–500 cm^{-1} wavenumber region with a resolution of 4 cm^{-1} and 32 scans. ^{1}H NMR spectroscopy were obtained on a Bruker AVANCE-III 500 MHz spectrometer at 25 °C, using deuteroxide (D_2O) as solvents. The cross-section of hydrogels was sprayed with gold and photographed by scanning electron microscopy (SEM, Hitachi S-8000) to obtain the internal morphology.

2.6. Determination of crosslinking efficiency

Ninhydrin-derivatized spectrophotometric assays were employed to determine the degree of effective crosslinking and unreacted amino groups during the coupling reaction [20]. In detail, Pec-ADH and lyophilized hydrogels were added to 1 mL of sodium acetate buffer (1 mol/L, pH = 5) and stirred at 400 rpm for 30 min to obtain a solution, followed by adding ninhydrin reagent. The mixtures were boiled for 30 min, then 75 mL of water/ethanol solution (v/v, 1:1) was added and incubated for 2 h at dark. The free amino groups were determined by

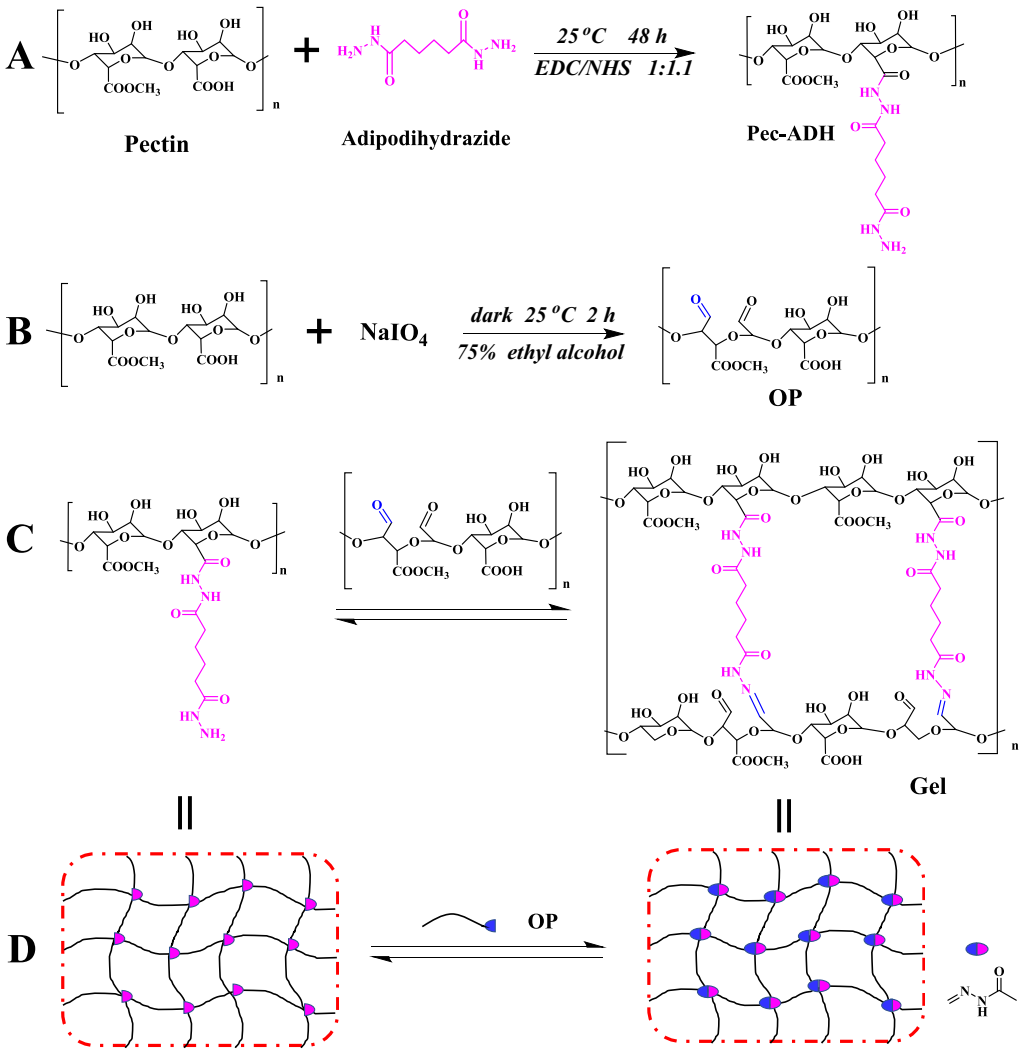

Fig. 1. Schematic illustration of the reaction in the present study. (A) Functionalization of pectin by adipodihydrazide, (B) Oxidization of pectin, (C) Synthesis of hydrogel, and (D) Schematic of the hydrogel.

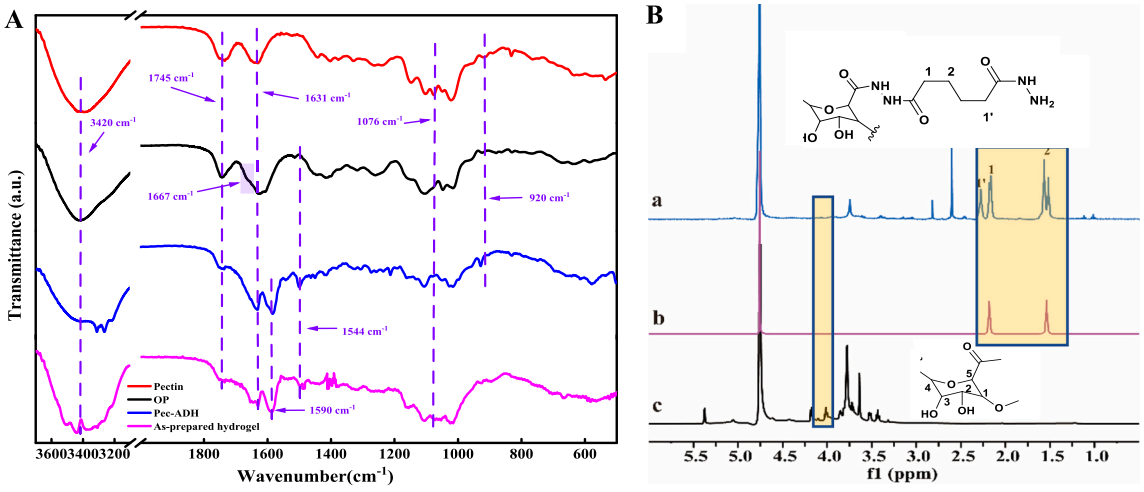

Fig. 2. (A) FTIR spectra of pectin, OP, Pec-ADH, and the as-prepared hydrogel. (B) ^{1}H NMR spectra of Pec-ADH (a), adipodihydrazide (b), and pectin (c).

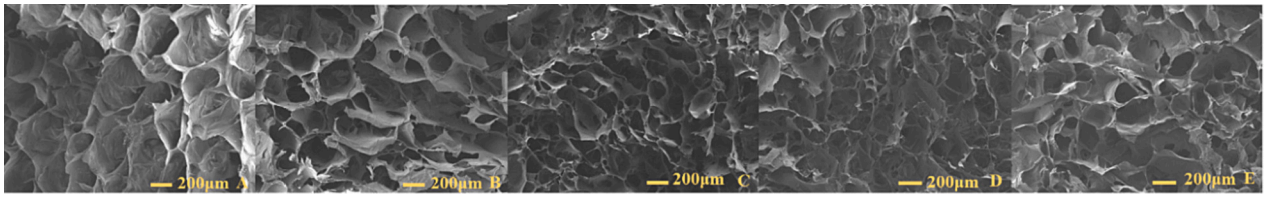

Fig. 3. SEM images (×50) of hydrogel with different fractions of feedstocks (A) Gel 1; (B) Gel 2; (C) Gel 3; (D) Gel 4; (E) Gel 5.

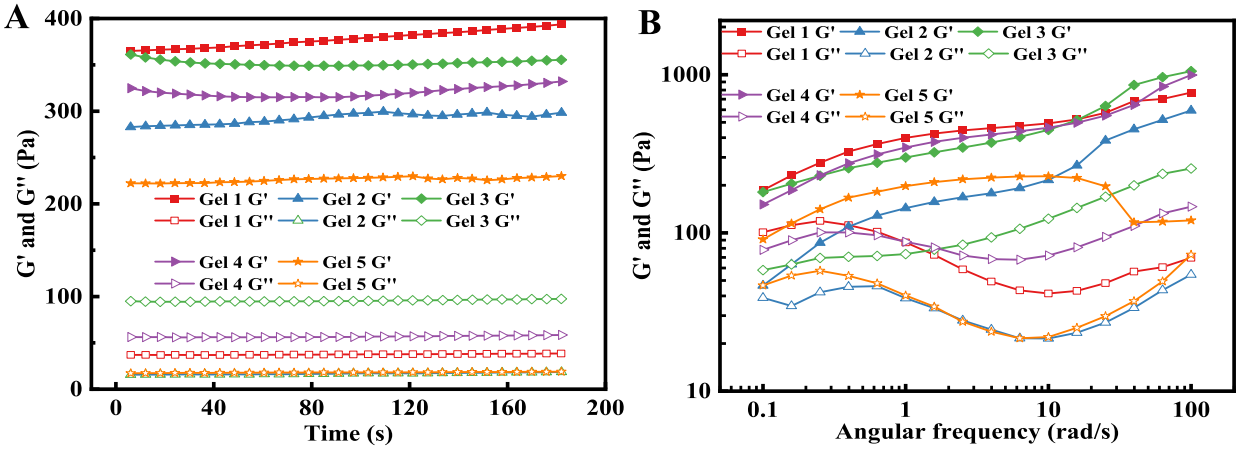

Fig. 4. Rheological properties of hydrogels. (A) Time sweep; (B) Frequency sweep.

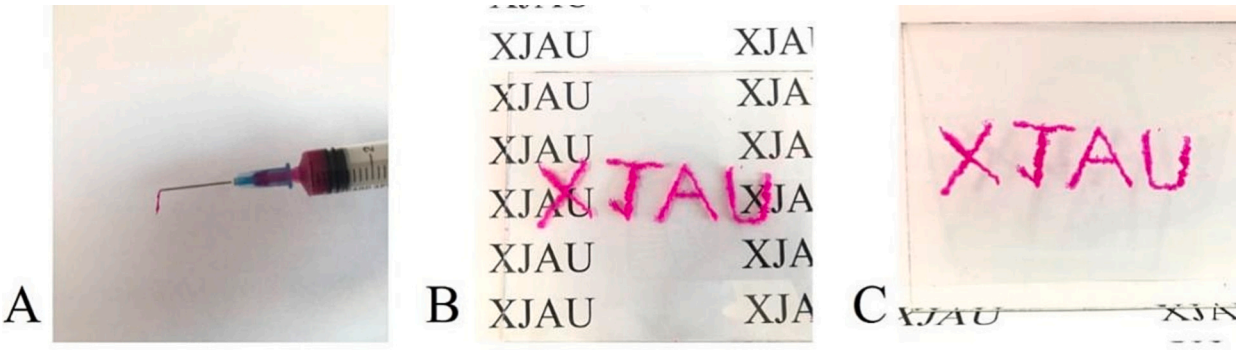

Fig. 5. Photograph of injectable performance. (A) Injection processes from an injector with a 0.45 mm needle; (B) Diagram of the writing of "XJAU"; (C) Fluidity of hydrogels on a vertical glass plate.

measuring the absorbance at 570 nm.

2.7. Rheological analysis

Discovery HR-2 rheometer (TA Instruments, USA) with a 20 mm parallel plate was used to perform the rheological experiments at 25 °C, and the gap was set as 1000 μm. The time sweep tests were performed to record the storage modulus and loss modulus of the gels at an angular frequency of 1 Hz and strain of 0.5 %. The mechanical properties of hydrogels were evaluated by scanning test with angular frequency in the range of 0.1–100 rad/s at a fixed strain of 0.5 %. Under a fixed angular frequency of 1 Hz, the strain sweep test (0.1–500 %) was used to determine the flow point. Then alternate step strain sweep was used to monitor the self-healing process of the hydrogels.

2.8. Macroscopical self-healing and injectable tests of the as-prepared hydrogels

The self-healing properties of hydrogels were also investigated through macroscopic self-healing tests [11]. In detail, the obtained hydrogels were cut into two parts, and half was stained with rhodamine B. At room temperature, the cut hydrogel was lightly touched on the petri dish and sealed with plastic wrap to prevent the evaporation of water. After a while, the gel was taken out, observed, and pulled in a direction perpendicular to the cutting line to determine whether the gel healed utterly. Moreover, the self-healing hydrogel was completely broken and placed in a starlike mold, which was covered by a wrap. The sample was taken out and observed for its integrity and smoothness.

The injectability test was conducted according to the published data with few modifications [21]. In detail, the OP and Pec-ADH solution was mixed in a 5 mL syringe. The hydrogel was pushed out from the 0.45 mm needle of the syringe onto the glass plate, during which the "XJAU" was written. Moreover, the glass plate was erected to determine the fluidity of the hydrogel by observing whether the word would be damaged.

2.9. Swelling properties of the hydrogel

The lyophilized hydrogel was weighed and immersed in distilled

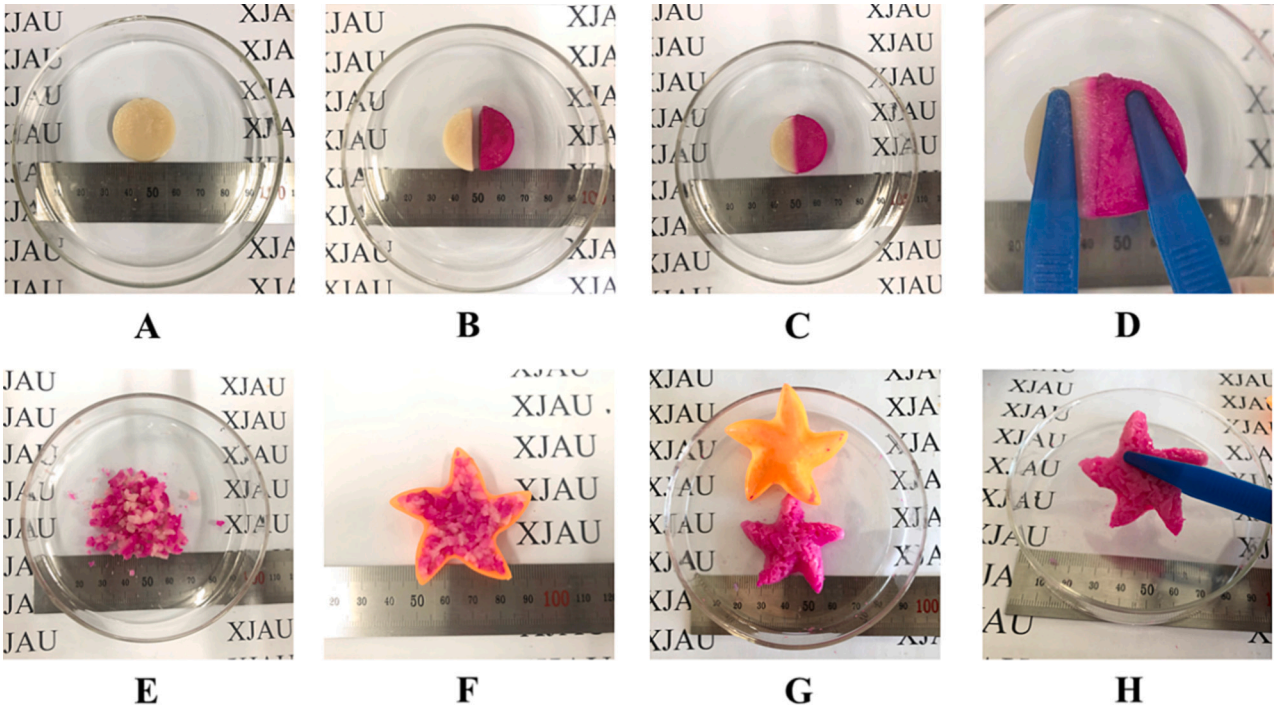

Fig. 6. Schematic of the macroscopic experiment for the self-healing performance of the hydrogels. (A) The original hydrogel. (B) The hydrogel was cut into two parts, one of which was stained with rhodamine B. (C) The hydrogel self-healed at 22 °C for 1.5 h without adding any chemicals. (D) The hydrogel was pulled in a direction perpendicular to the cut line to observe its self-healing properties. (E) The self-healed hydrogel was recut up to granules. (F) The granules were left in a stellated mold. (G) The self-healed hydrogel was removed from the mold. (H) Final self-healed hydrogel.

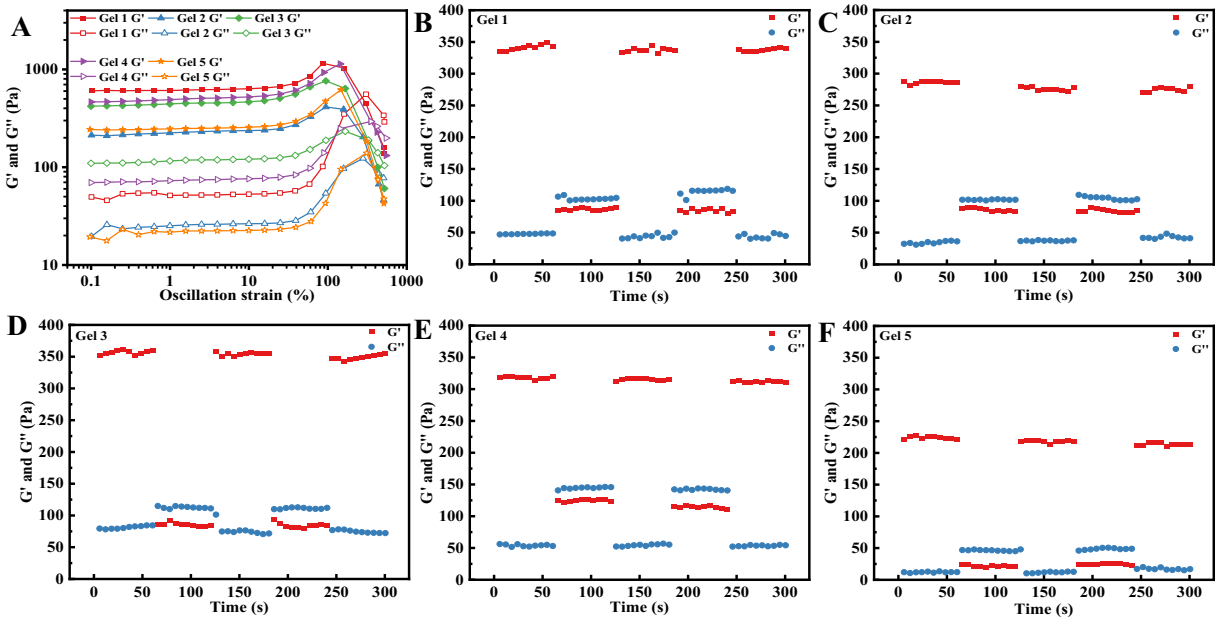

Fig. 7. Rheological characterization of self-healing properties. (A) Oscillation strain sweep (0.1–500 %); G' and G" values of the (B) Gel 1, (C) Gel 2, (D) Gel 3, (E) Gel 4, (F) Gel 5 in continuous step measurements.

water at 37 °C. It was taken out at regular intervals and weighed by drying the excess water on the surface with absorbent paper. This process was terminated till the equilibrium swelling was reached. The swelling ratios of hydrogels at different time intervals were calculated by Eq. (1).

$$SR(\%) = \left[(w_s - w_d)/w_d \right] \times 100 \quad (1)$$

where W_s and W_d are the weight of the swollen and lyophilized hydrogels, respectively.

2.10. pH-responsiveness of the hydrogels

Due to the wide existence of carboxyl functional groups in the pectin molecules, the pectin-based hydrogel generally presented pH-responsiveness. Thus, we determined the pH-responsiveness by

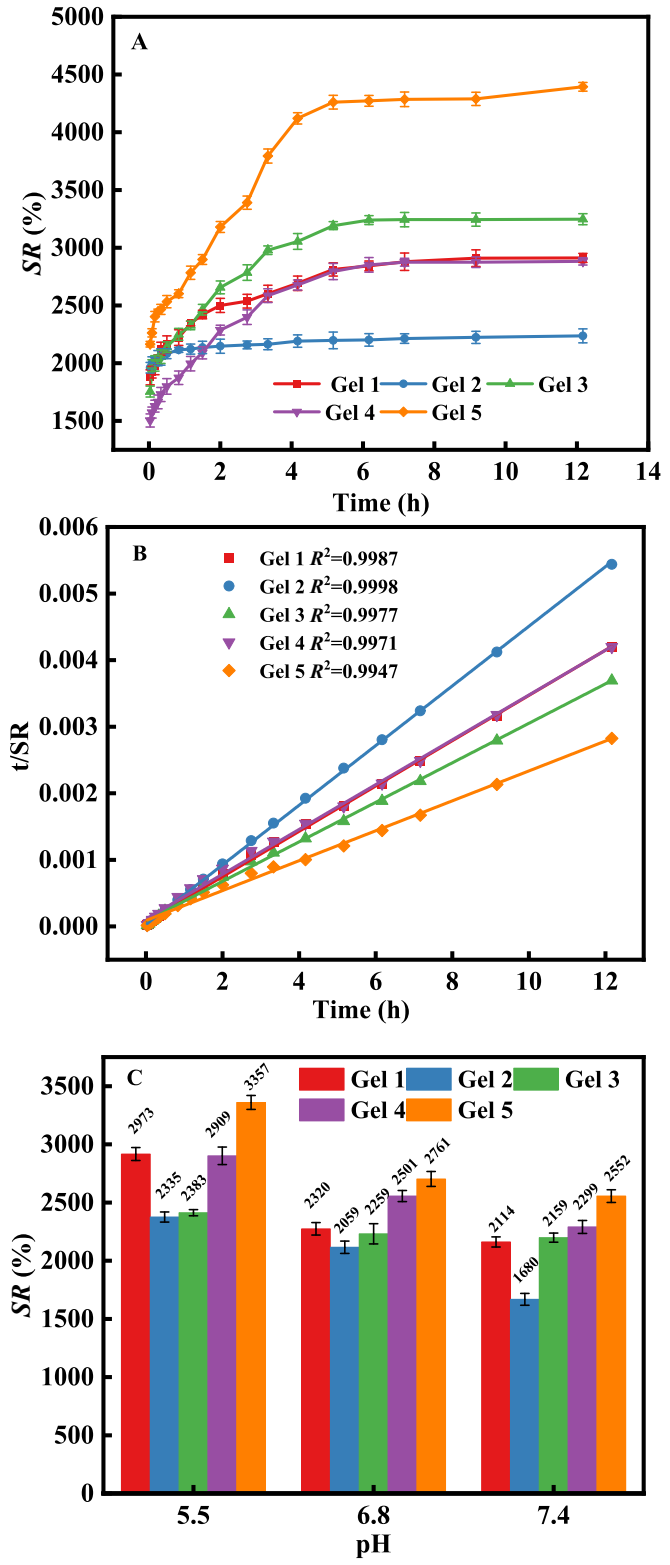

Fig. 8. The swelling ratio of the as-prepared hydrogels in different media. (A) The swelling ratio of hydrogel in deionized water. (B) Fitting of the second-order kinetics model. (C) The swelling ratio of the as-prepared hydrogels in PBS with different pH values (5.5, 6.8, and 7.4) for 6 h.

measuring the change in the swelling ratio of as-prepared hydrogels in an aqueous solution under different conditions. The lyophilized hydrogels were immersed in KH_2PO_4-Na_2HPO_4 buffer solutions (PBS) with different pH values (5.5, 6.8, and 7.4) for 6 h at room temperature. The weights of lyophilized and saturated hydrogels were used to determine the swelling ratio according to Eq. (1), and the variation of the obtained swelling ratio was in line with the responsiveness.

2.11. In vitro sustained release performance of hydrogels and kinetic study

To enhance the dispersion of 5-FU in the network of acylhydrazone-derived whole pectin-based injectable hydrogel, in situ loading was performed. In detail, the distilled water was just replaced by the 2.5 mL of 5-FU solution (100 mg/L), and all the other operations were according to the preparation of injectable hydrogel. The resultant 5-FU loaded hydrogels were noted as Gel 1-D, Gel 2-D, Gel 3-D, Gel 4-D, and Gel 5-D, according to the serial number of hydrogels shown in Table 1. Moreover, the dose of 5-FU was attempted to be reduced in the present study due to the well-known side effects. The loading efficiency was 0.25 mg/0.2 g (i.e., 0.125 %) which was calculated by Eq. (2).

$$\text{Loading efficiency } (\%) = \frac{(Total\ \text{drug}) - (Free\ \text{drug})}{Weight\ of\ carriers} \times 100 \quad (2)$$

The in vitro release of 5-FU from the pectin-based drug delivery system was performed at 37 °C in 10 mL of the release media (i.e., PBS) with different pH (6.8 and 7.4). To determine the cumulative release ratio, 1 mL of the simulated release media was sucked out at preset time intervals, which further measured its absorbance at 266 nm. In this process, the sucked samples were first centrifuged at 10000 rpm for 5 min and then filtered by a microfilter membrane (0.22 μm) to remove the pectin-derived hydrogel. After each sampling, 1 mL of the original PBS was added to the release media immediately to maintain the dynamic balance of the simulation environment. The cumulative release ratio was calculated by Eq. (3).

$$Q = \frac{C_n \times V_0 + V_i \sum_{i=1}^{n-1} C_i}{m} \quad (3)$$

where Q is the cumulative release ratio, the C_n (mg/L) represented the concentration of 5-FU in the release media after the *nth* sampling, the V_0 and V_i were the volumes of the release media and sampling, the C_i (mg/L) was the 5-FU concentration at the *ith* sampling, and m (mg) was the total dosage of 5-FU loaded in the as-prepared hydrogels.

The kinetics studies were employed to describe the release behavior of 5-FU from the as-prepared hydrogels. Three commonly used models were selected to explore drug release mechanisms, including the First order model (Eq. (4)), Higuchi model (Eq. (5)), and Ritger-Peppas model (R-P) (Eq. (6)).

$$-ln(1-Q) = k_1 t \quad (4)$$

$$Q = k_2 t^{0.5} \quad (5)$$

$$lnQ = nlnt + lnk_3 \quad (6)$$

where Q was the drug release ratio at different time intervals according to the determination of cumulative release ratio, K_i ($i = 1, 2, 3$) was the kinetic constant of the three models, and n was the diffusion index used to determine the diffusion mechanism.

2.12. Cellular compatibility of the as-prepared hydrogels

The cytocompatibility of hydrogel was measured by MTT colorimetric method using mouse fibroblast cell lines (L929). L929 cell suspensions (100 μL, 8×10^4/mL) were placed in 96-well cell culture plates and further cultured for 12 h at 37 °C under 5 % CO_2. Then, 100 μL of hydrogel-contained solutions with different concentrations (3.6, 1.8, 0.9, 0.45, and 0.225 mg/mL) were prepared as MEM media and added into the above-mentioned wells, and the L929 cell lines were continued

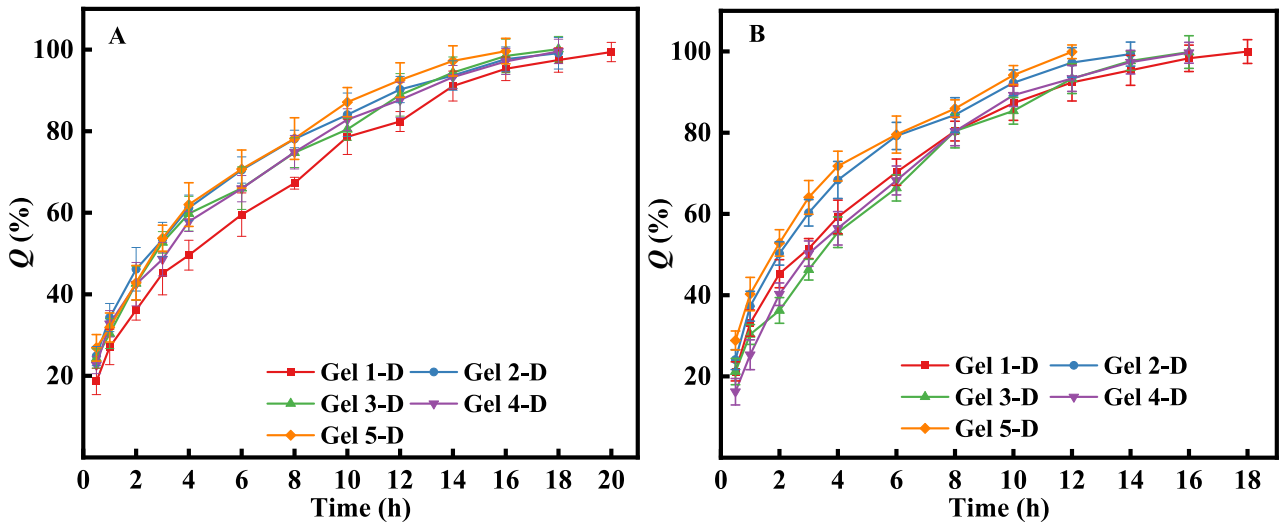

Fig. 9. Drug release in different simulated environments. (A) dilute acidic condition with a pH of 6.8; (B) dilute alkaline condition with a pH of 7.4.

Table 2
Kinetic model parameters of the first-order, Higuchi, Bhaskar, and Ritger-Peppas models in the simulated media of pH = 6.8 and 7.4.

		pH = 6.8					pH = 7.4				
		Gel 1	Gel 2	Gel 3	Gel 4	Gel 5	Gel 1	Gel 2	Gel 3	Gel 4	Gel 5
The First order model	k_1	0.1260	0.1676	0.1542	0.1469	0.1799	0.1873	0.2746	0.2011	0.1940	0.2406
	R_1^2	0.9974	0.9897	0.9947	0.9945	0.9908	0.9909	0.9358	0.9866	0.9868	0.9760
The Higuchi model	k_2	22.32	23.70	23.64	22.83	23.97	25.22	25.89	27.48	26.81	24.98
	R_2^2	0.9988	0.9985	0.9969	0.9988	0.9974	0.9969	0.9859	0.9975	0.9967	0.9772
The Bhaskar model	K_4	0.3319	0.4382	0.4048	0.38519	0.4701	0.4891	0.7093	0.5236	0.5052	0.5971
	R_4^2	0.9822	0.9584	0.9722	0.9699	0.9591	0.9570	0.8818	0.9463	0.9467	0.9519
The Ritger-Peppas model	n	0.4350	0.4084	0.2694	0.4057	0.4018	0.4410	0.4203	0.4154	0.4910	0.3835
	K_3	28.02	32.61	30.71	31.51	33.91	31.26	35.86	26.62	27.65	39.84
	R_3^2	0.9999	0.9995	0.9993	0.9988	0.9994	0.9984	0.9924	0.9978	0.9984	0.9898

to be cultured at 37 °C under 5 % CO_2 for different times (24 h, 48 h, and 72 h). MTT solution (100 μL, 1 mg/mL) was added to each well and cultured for another 4 h for staining the L929 cell lines. Finally, 150 μL of DMSO was added. A BIV-TEK INSTRUMENTS INC was used to measure the absorbance (OD) of each well at 570 nm. The cell proliferation ratio (CPR, %) was calculated as Eq. (7).

$$\mathrm{CPR}(\%) = \frac{\textit{The OD value of the sample}}{\textit{The OD value of the control group}} \times 100 \quad (7)$$

2.13. Cancer cell inhibitory effect of the 5-FU-loaded hydrogels

Breast cancer cells lines (MCF-7) were used to investigate the inhibitory effect of the 5-FU-loaded hydrogels. In this process, the culture time of the MCF-7 after adding 5-FU-loaded hydrogels was 12 h and 24 h. All the other operations were performed according to the cytocompatibility assays. The cancer cell inhibitory rate was also calculated according to Eq. (7).

3. Results and discussion

3.1. Characterization

FT-IR was used to elucidate the chemical structure of pectin, OP, Pec-ADH, and the obtained hydrogel (Fig. 2A). The present peaks at 3420 cm^{-1}, 1745 cm^{-1}, and 1631 cm^{-1} were ascribed to the hydroxyl functional group, carboxylate carbonyl group, and ester carbonyl group [22,23]. The C—O stretching vibration of secondary alcohol in the d-galacturonic acid unit can be found at 1076 cm^{-1} in the spectra of pectin and Pec-ADH but significantly whacked in the curve of OP and the as-prepared hydrogel. Compared with the spectra of pectin, there was a shoulder peak at 1667 cm^{-1} in the OP curve which indicated the generation of formyl groups [18]. The peaks located at 1076 cm^{-1} and 920 cm^{-1} were ascribed to the bending vibration of hydroxyl groups in the carboxyl functional groups, and the signal of the two characteristic peaks slightly changed after the modification by diacylhydrazine adipate [24]. The newly generated peaks at 1590 cm^{-1} and 1544 cm^{-1} were ascribed to the stretching vibration of the carbonyl and in-plane bending vibration of secondary amine in the hydrazide groups [25,26]. Moreover, a clear split was found in the spectra of Pec-ADH at 3420 cm^{-1}, which was induced by acylhydrazine groups [27]. All these results indicated the successful synthesis of Pec-ADH. In the spectra of acylhydrazone-derived whole pectin-based hydrogel, the peak around 3420 cm^{-1} was further split, which may be due to the strong conjugation of acylhydrazone groups. Additionally, other peaks were the same as in the Pec-ADH spectra, indicating the successful synthesis based on acylhydrazone linkage.

NMR spectroscopy can provide detailed information about the proton environment of the samples. Fig. 2B-c showed a ^{1}H NMR spectrum of pectin. The sharp singlet at 3.75 ppm was responsible for the protons in the methoxy groups (i.e., -$COOCH_3$) [28]. The protons linked on the C2 and C3 were found at 3.92 ppm and 4.05 ppm [29] that almost disappeared at the ^{1}H NMR spectrum of Pec-ADH (Fig. 2B-a), indicating the successful periodate oxidation. The spectrum of Pec-ADH showed the signals at 2.28, 2.15, and 1.54 ppm (Fig. 2B-a), which were the protons vested in ADH (Fig. 2B-b) [30]. These results meant that the ADH was successfully conjugated onto the pectin chain.

The morphology of the as-prepared hydrogels was observed by SEM technique, and the results are shown in Fig. 3. It was clear that all the samples showed a more uniform pore structure than pectin-chitosan

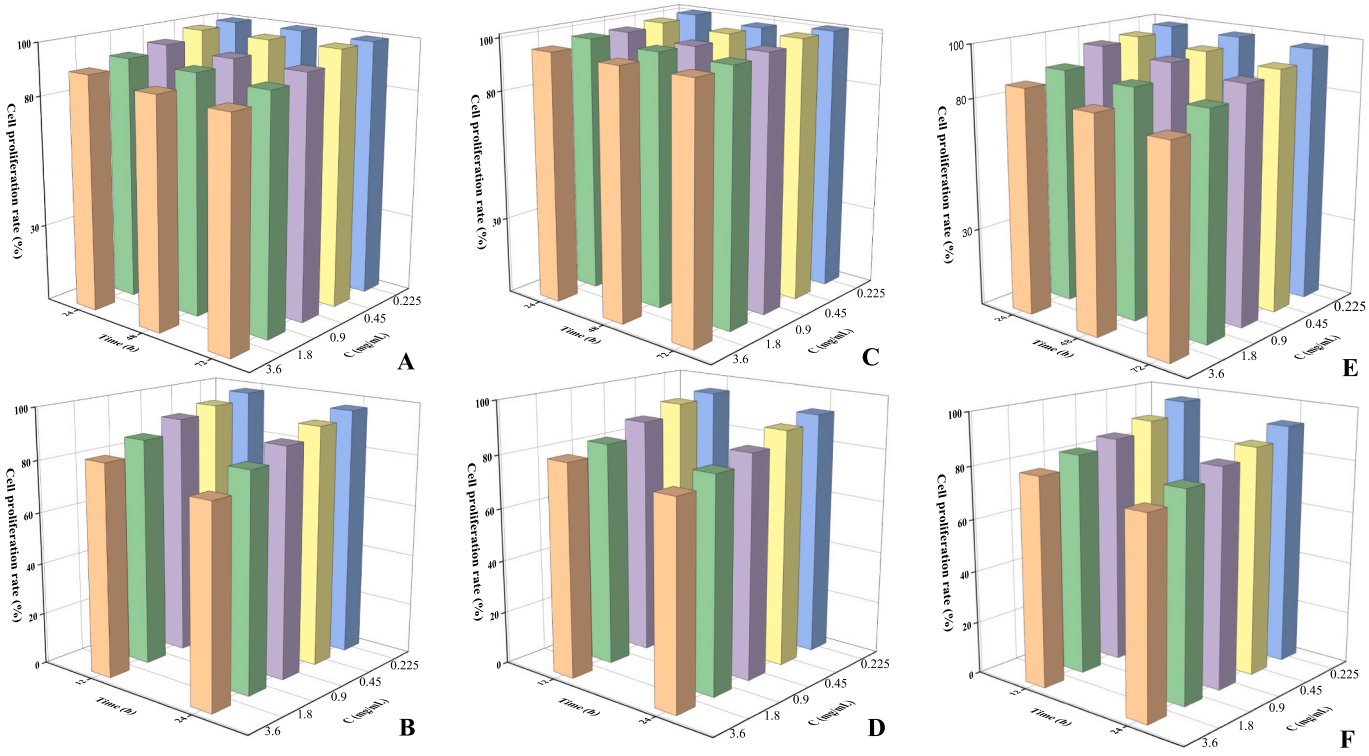

Fig. 10. The cellular compatibility of hydrogels and inhibitory effect of drug delivery systems on cancer cells via the MTT method. (A) L929 cell culture with Gel 3; (B) MCF-7 cell culture with Gel 3; (C) L929 cell culture with Gel 4; (D) MCF-7 cell culture with Gel 4; (E) L929 cell culture with Gel 5; (F) MCF-7 cell culture with Gel 5.

hybrid hydrogel [11]. It may be due to the higher solubleness of pectin and pectin derivatives than chitosan [31]. Moreover, the pore diameter presented an increasing trend with the oxidation degree of pectin, as shown in Figs. 3A–C. Figs. 3C, D, and E also presented a rising trend in the aperture with the increasing dosage of OP. All the results indicated the decisive effect of the oxidation degree on the pore structure that significantly influenced the swelling behavior and the consequent drug release performance.

3.2. Mechanical properties of the hydrogels

The oxidization induced the cleavage of C2-C3 linkages of the d-galacturonic acid units, which caused a change in the rigidity of the pectin chain [32]. As a result, the obtained hydrogel prepared from different OP will show the difference in the mechanical properties. To study the effect of the mass ratio of Pec-ADH to OP on the mechanical behavior of hydrogel, the storage modulus G' and loss modulus G" of hydrogel was measured with the change in time.

The G' were higher than G" (Fig. 4A), which indicated that all the samples were self-healing elastomers. Gel 1, Gel 2, and Gel 5 showed a decreased trend in G', indicating that the higher degree of oxidation contributed to the fluidity. A similar result can be obtained by comparing the G' of Gel 3, Gel 4, and Gel 5. These results can be explained by that the flexible OP molecules favored the flexibility of the crosslinked hydrogel. Moreover, the G' of the hydrogel decreased from 375 Pa to 225 Pa with the increased oxidation degree of pectin (Fig. 4A). These results were much higher than the Ca^{2+} crosslinked pectin-based hydrogel [33], indicating the stimulative role of covalent crosslinking on the mechanical properties. An et al. developed injectable hydrogels from OP and poly(N-isopropylacrylamide-*stat*-acylhydrazide) and obtained a similar G' toward the present study [17]. These results stated that the OP was a candidate for the preparation of injectable hydrogel.

Fig. 4B displays the rheological properties of all the hydrogels with different chemical constitutions under dynamic oscillation measurements. All the G' were larger than G" of the hydrogel regardless of the mass ratio of Pec-ADH to OP, indicating that the elastic module played a dominant role in the system rather than the viscous module. Moreover, the viscoelasticity of the gels significantly depended on the angular frequency, and the solid characteristic presented at a higher angular frequency (Fig. 4B), which was considered identity as the shape adaptive hydrogel [34]. These results showed that the as-prepared gels have both liquid-like mobility and solid-like elasticity. When the experiments were performed at a low angular frequency, the gels presented fluid characteristics, indicating the well-injectable performance.

3.3. Injectability and self-healing properties of hydrogels

The injection test from the syringe was performed, and the results are shown in Fig. 5. It can be seen that the hydrogel can be injected out from the needle without blocking (Fig. 5A). The word "XJAU" can be written smoothly on the glass plate (Fig. 5B). Moreover, the hydrogel did not flow down when the glass plate was vertical (Fig. 5C), indicating the forming of hydrogel after extruding from the syringe [12,35,36]. The phenomena that were shown in Fig. 5 also confirmed the great injectability of the acylhydrazone-derived whole pectin-based hydrogel.

The injection of hydrogel from the needle was generally classified into the damage and self-healing processes. Thus, the self-healing performance was one essential property of the injectable hydrogel. The macroscopic test was one of the characterizations that can reflect the self-healing performance, which was consequently performed in the present study, and the results are shown in Fig. 6. It was evident that Rhodamine B diffused from the stained part to the unstained part at the position of the cut line (Fig. 6C and D). Moreover, the self-healing hydrogel can maintain its integrity after pulling (Fig. 6D). These results showed the well self-healing performance of the acylhydrazone-derived whole pectin-based hydrogel [3,37–39]. The shredding-self-healing cycle also showed the desired result that the granules can self-heal into an entirety at 22 °C for 1.5 h without adding any chemicals

(Fig. 6E–H). Compared with the self-healing cellulose-based hydrogel via acylhydrazone, the acylhydrazone-derived whole pectin-based hydrogel showed a much short self-healing time (24 h vs. 1.5 h) [40]. This phenomenon again indicated that pectin was suitable for the preparation of self-healing hydrogels.

In order to assess the self-healing properties of hydrogels, the continuous step strain experiment was performed. Fig. 7A showed that the G' were lower than the G" in all the hydrogel at 400 % strain, indicating that the hydrogel network was disrupted from a gel state to a quasi-liquid state. Similar results can be obtained from the published data that studied the OP-based injectable hydrogel [17]. As shown in Fig. 7(B–F), when the strain was increased from 1 % to 400 %, the G' was significantly lower than the G", indicating damage to the gel network. When the strain returned to 1 %, the G' could return to the initial value immediately, implying the efficient self-healing of the hydrogel network. These data demonstrate the excellent self-healing properties of pectin-based hydrogels based on acylhydrazone bonds.

3.4. Swelling properties of hydrogel in different media

Fig. 8A showed the change in the swelling ratio of as-prepared hydrogels in deionized water with the extent of swelling time. All the samples reached equilibrium swelling in 6 h, and the swelling ratios were 2897.20 %, 2236.90 %, 3293.81 %, 2902.67 %, and 4306.65 % for gels 1–5, respectively. Moreover, the swelling ratio of gel 5 was much higher than that of gel 1 and 2. The crosslinking efficiency of the gels 1–5 were 92.3 %, 93.6 %, 93.1 %, 95.7 %, and 96.2 %, indicating that the crosslinking density from large to small should be Gel 5 > Gel 2 > Gel 1 and Gel 5 > Gel 4 > Gel 3. However, the swelling ratio showed irregular trends (i.e., Gel 5 > Gel 1 > Gel 2, Gel 5 > Gel 3 > Gel 4, and Gel 5 > Gel 3 > Gel 1 ≈ Gel 4 > Gel 2). It is clear that the hydrogels formed from OP5 that had the highest degree of oxidization showed better swelling properties. This phenomenon can be explained by that (1) the crosslinking reaction formed a 3D network that endowed the hydrogels with expandability without destruction; (2) as a hydrophilic component, the flexibility OP5 was the best, which contributed to the movement of pectin molecules and the consequent expandability swelling ratio; (3) the decrease content of hydroxyl group reduced the content of hydrogen bonding, which increased the number of the exposed carboxyl group, a functional group that could form hydration.

We employed second-order kinetic model to study the swelling behavior in the present study, and the results are shown in Fig. 8B. It is evident that all the R^2 values of the model were higher than 0.99. These results indicated that hydrogen bonding and other secondary valence forces existed among different chains, and the interchain secondary valence bonds were broken with the penetration of the water molecules [41]. Moreover, it was an entropy-driven process in which the cleavage of interchain secondary valence bonding allowed the expandability of polymer networks to accommodate the influx of water through the relaxation of the stresses produced by osmotic pressure [42].

Fig. 8C presented the swelling ratio of the as-prepared hydrogels in PBS with different pH values (5.5, 6.8, and 7.4) for 6 h. The swelling ratio showed a significant decreasing trend with the increasing pH values, indicating the pH-responsiveness of the as-prepared hydrogels. It was induced by the dissociation of the carboxyl groups under different pH conditions [43]. In detail, the higher pH condition contributed to the dissociation of carboxyl groups to carboxylate ions, which can be linked by the salt bridge (Na^+) to form a coulomb force-driven network, and the corresponding hydrogel showed a lower swelling ratio. Moreover, the swelling ratios of hydrogels in PBS were lower than those in distilled water. It also proved the role of the salt bridge in forming the hydrogel network [44]. In this process, the pH-responsiveness of acylhydrazone groups also played an important role. Under acidic conditions, the N atom was the proton receptor, which increased the hydrophilicity of the hydrogel and facilitated the entry of water molecules, thus showing a higher swelling degree [45,46].

3.5. In vitro drug release performance and kinetics studies

In this study, the 5-FU was used as the model drug, and the sustained release performance of acylhydrazone-derived whole pectin-based injectable hydrogel drug delivery system was studied. As shown in Fig. 9, the 5-FU was gradually released in the simulated environment without sudden release. It can be seen that the slow-release system has a good in vitro release effect in both simulated environments and the drug can be continuously released within 12 h. The cumulative release ratio was more than 75 % at a pH of 6.8 and more than 80 % at a pH of 7.4, respectively. These results corresponded to the swelling study. An et al. have prepared injectable and biodegradable self-healing hydrogel from OP and poly (N-isopropylacrylamide-*stat*-acylhydrazide) (OP/NIPAm) and obtained better results, compared with the present study [17]. Oppositely, Yang et al. obtained caseinate-reinforced pectin composite hydrogels [47] that presented a much high release rate than OP/NIPAm [17] and acylhydrazone-derived whole pectin-based hydrogel in the present study. This result indicated the importance of the hydrophilia of the feedstock, viz., the hydrophilia of the carriers influenced the contact between the release media and carriers and consequently determined the diffusion of the drug model from the inner to the outside. Moreover, the acylhydrazone-derived whole pectin-based hydrogel in the present study showed a similar result compared with the carrier from OP/chitosan [12]. In vitro release studies showed that the hydrogels had good properties and could be used as a candidate for drug loading.

Four kinetic models were fitted to study the release behavior, and the results are listed in Table 2. The R^2 values of the First order, Higuchi, and Ritger-Peppas models were all higher than 0.98 under both acidic and alkaline conditions, indicating the well-fitting toward the experimental data. These results manifested that the release of 5-FU from hydrogel-based drug delivery systems was related to the loading drug concentration in the hydrogel and based on the Fickian diffusion [41,42]. For all the drug delivery systems, the n values from the Ritger-Peppas model were less than 0.5, indicating the Fickian diffusion transport process [12]. Moreover, the main force that controlled the drug release was the diffusion of water molecules rather than the relaxation of the macromolecular chain, which could also explain why the hydrogels swelled while preventing the sudden release of drugs [48].

3.6. The cellular compatibility of hydrogels and inhibitory effect of drug delivery systems on cancer cells

Gel 3, Gel 4, and Gel 5 were selected to study the cellular compatibility and inhibitory effect of cancer cells. All the assays were performed via the MTT method, and the results are shown in Fig. 10. The cytocompatibility assay showed that the higher hydrogel concentration induced a lower cell proliferation ratio. The lowest cell proliferation ratio was 85.82 % ± 1.87 %, and the highest was 100.84 % ± 0.71 % at 24 h. When cultured for 72 h, the lowest cell proliferation ratio was 78.02 % ± 2.11 %, and the highest was 101.43 % ± 2.54 %. We also found that the cell proliferation ratio slightly decreased with the increased degree of oxidation of OP, indicating the mild side effect of formyl groups. Moreover, the present study selected a much higher concentration than the published data [49,50], but an excellent result was obtained. These results of cytocompatibility showed that the acylhydrazone-derived whole pectin-based hydrogel showed good cellular compatibility.

In the assay on the inhibition of cancer cells (MCF-7), it was found that the drug-loaded hydrogel had an inhibitory effect on cancer cells, and the inhibitory effect on MCF-7 enhanced with the increasing concentration of hydrogels, i.e., the dosage of 5-FU. The inhibition of MCF-7 cell lines for 24 h showed that the cell proliferation ratios with Gel 3, Gel 4, and Gel 5 were all below 80 %. It seemed to be a poor result but was limited by the selected dosage of 5-FU (4.5 μg/mL), which was much lower than the clinical medication (~15 mg/kg·day) and published data [51,52]. Combined with the slow-release performance and ultra-low

dose of the 5-FU, the drug release system obtained in the present study manifested an excellent inhibitory effect on MCF-7 cell lines.

4. Conclusion

The present work showed an acylhydrazone-derived whole pectin-based hydrogel as an injectable drug delivery system. The hydrogel presented injectable performance and showed excellent self-healing properties within 1.5 h. The swelling ratio can be as high as 4306.65 % in distilled water, and the swelling ratios of the as-prepared hydrogels correspond to the oxidation degree of pectin (i.e., the content of the formyl group). The results in stimuli-responsiveness of as-prepared hydrogel showed significant salt- and pH-responsiveness, which was significantly influenced by the surface functional groups. 5-FU can be released from the drug delivery systems for more than 12 h without sudden release. The kinetics studies showed that the diffusion of water molecules controlled the drug release rather than the relaxation of the macromolecular chain. Moreover, the cellular compatibility and inhibitory effect on cancer cell lines manifested excellent performance. Overall, the acylhydrazone-derived whole pectin-based hydrogel was an excellent candidate for injectable drug delivery systems.

CRediT authorship contribution statement

Shu-ya Wang: Conceptualization, Methodology, Investigation, Data curation, Writing – original draft. **Maryamgul Tohti:** Conceptualization, Methodology, Investigation, Data curation, Writing – original draft. **Jia-qi Zhang:** Formal analysis, Visualization, Methodology, Investigation. **Jun Li:** Methodology, Formal analysis, Supervision, Project administration. **De-qiang Li:** Conceptualization, Validation, Project administration.

Declaration of competing interest

The authors declare no competing financial interests.

Data availability

Data will be made available on request.

Acknowledgment

The present work was supported by the Natural Science Foundation of Xinjiang Uygur Autonomous Region, China (NO. 2021D01A74), National Natural Science Foundation of China (NO. 32160352), Xinjiang Key Laboratory of Agricultural Chemistry and Biomaterials of the Xinjiang Agricultural University (NO. KF202201), Tianshan Talents Program of Xinjiang, China (2021−2023) (NO. 2021267), and Postgraduate Innovation Project of Xinjiang Agricultural University (NO. XJAUGRI2022048).

References

[1] Z. Mazidi, S. Javanmardi, S.M. Naghib, Z. Mohammadpour, Smart stimuli-responsive implantable drug delivery systems for programmed and on-demand cancer treatment: An overview on the emerging materials, Chem. Eng. J. 433 (2022), 134569, https://doi.org/10.1016/j.cej.2022.134569.

[2] E. Utomo, S.A. Stewart, C.J. Picco, J. Domínguez-Robles, E. Larrañeta, Classification, material types, and design approaches of long-acting and implantable drug delivery systems, in: E. Larrañeta, T. Raghu Raj Singh, R. F. Donnelly (Eds.), Long-Acting Drug Delivery Systems, Woodhead Publishing, 2022, pp. 17–59, https://doi.org/10.1016/B978-0-12-821749-8.00012-4.

[3] Z. Wang, Y. Zhang, Y. Yin, J. Liu, P. Li, Y. Zhao, D. Bai, H. Zhao, X. Han, Q. Chen, High-strength and injectable supramolecular hydrogel self-assembled by monomeric nucleoside for tooth extraction wound healing, Adv. Mater. (2022) 2108300, https://doi.org/10.1002/adma.202108300.

[4] S.V. Popov, G.Y. Popova, I.R. Nikitina, P.A. Markov, D.S. Latkin, V.V. Golovchenko, O.G.A. Patova, N. Krachkovsky, V.V. Smirnov, E.A. Istomina, K.V. Shumikhin, A. A. Burkov, E.A. Martinson, S.G. Litvinets, Injectable hydrogel from plum pectin as a barrier for prevention of postoperative adhesion, J. Bioact. Compat. Polym. 31 (5) (2016) 481–497, https://doi.org/10.1177/0883911516637374.

[5] X. Ding, G. Li, P. Zhang, E. Jin, C. Xiao, X. Chen, Injectable self-healing hydrogel wound dressing with cysteine-specific on-demand dissolution property based on tandem dynamic covalent bonds, Adv. Funct. Mater. 31 (19) (2021) 2011230, https://doi.org/10.1002/adfm.202011230.

[6] Y. Li, H.Y. Yang, D.S. Lee, Advances in biodegradable and injectable hydrogels for biomedical applications, J. Control. Release 330 (2021) 151–160, https://doi.org/10.1016/j.jconrel.2020.12.008.

[7] X. Su, W. Xie, P. Wang, Z. Tian, H. Wang, Z. Yuan, X. Liu, J. Huang, Strong underwater adhesion of injectable hydrogels triggered by diffusion of small molecules, Mater. Horiz. 8 (8) (2021) 2199–2207, https://doi.org/10.1039/D1MH00533B.

[8] T.E.L. Douglas, M. Dziadek, J. Schietse, M. Boone, H.A. Declercq, T. Coenye, V. Vanhoorne, C. Vervaet, L. Balcaen, M. Buchweitz, F. Vanhaecke, F. Van Assche, K. Cholewa-Kowalska, A.G. Skirtach, Pectin-bioactive glass self-gelling, injectable composites with high antibacterial activity, Carbohydr. Polym. 205 (2019) 427–436, https://doi.org/10.1016/j.carbpol.2018.10.061.

[9] Y. Shitrit, M. Davidovich-Pinhas, H. Bianco-Peled, Shear thinning pectin hydrogels physically cross-linked with chitosan nanogels, Carbohydr. Polym. 225 (2019), 115249, https://doi.org/10.1016/j.carbpol.2019.115249.

[10] S. Bernhard, M.W. Tibbitt, Supramolecular engineering of hydrogels for drug delivery, Adv. Drug Deliv. Rev. 171 (2021) 240–256, https://doi.org/10.1016/j.addr.2021.02.002.

[11] D. Li, S. Wang, Y. Meng, Z. Guo, M. Cheng, J. Li, Fabrication of self-healing pectin/chitosan hybrid hydrogel via Diels-Alder reactions for drug delivery with high swelling property, pH-responsiveness, and cytocompatibility, Carbohydr. Polym. 268 (2021), 118244, https://doi.org/10.1016/j.carbpol.2021.118244.

[12] D.-Q. Li, S.-Y. Wang, Y.-J. Meng, J.-F. Li, J. Li, An injectable, self-healing hydrogel system from oxidized pectin/chitosan/gamma-Fe_2O_3, Int. J. Biol. Macromol. 164 (2020) 4566–4574, https://doi.org/10.1016/j.ijbiomac.2020.09.072.

[13] X. Ji, H. Shao, X. Li, M.W. Ullah, G. Luo, Z. Xu, L. Ma, X. He, Z. Lei, Q. Li, X. Jiang, G. Yang, Y. Zhang, Injectable immunomodulation-based porous chitosan microspheres/HPCH hydrogel composites as a controlled drug delivery system for osteochondral regeneration, Biomaterials 285 (2022), 121530, https://doi.org/10.1016/j.biomaterials.2022.121530.

[14] A.S. Prasad, J. Wilson, L.V. Thomas, Designer injectable matrices of photocrosslinkable carboxymethyl cellulose methacrylate based hydrogels as cell carriers for gel type autologous chondrocyte implantation (GACI), Int. J. Biol. Macromol. 224 (2023) 465–482, https://doi.org/10.1016/j.ijbiomac.2022.10.137.

[15] M. Li, Q. Tu, X. Long, Q. Zhang, H. Jiang, C. Chen, S. Wang, D. Min, Flexible conductive hydrogel fabricated with polyvinyl alcohol, carboxymethyl chitosan, cellulose nanofibrils, and lignin-based carbon applied as strain and pressure sensor, Int. J. Biol. Macromol. 166 (2021) 1526–1534, https://doi.org/10.1016/j.ijbiomac.2020.11.032.

[16] T.M. Almutairi, H.H. Al-Rasheed, M. Monier, F.S. Alatawi, N.H. Elsayed, Synthesis and characterization of photo-crosslinkable cinnamate-functionalized pectin, Int. J. Biol. Macromol. 210 (2022) 208–217, https://doi.org/10.1016/j.ijbiomac.2022.04.109.

[17] H. An, Y. Yang, Z. Zhou, Y. Bo, Y. Wang, Y. He, D. Wang, J. Qin, Pectin-based injectable and biodegradable self-healing hydrogels for enhanced synergistic anticancer therapy, Acta Biomater. 131 (2021) 149–161, https://doi.org/10.1016/j.actbio.2021.06.029.

[18] B. Gupta, M. Tummalapalli, B.L. Deopura, M.S. Alam, Functionalization of pectin by periodate oxidation, Carbohydr. Polym. 98 (1) (2013) 1160–1165, https://doi.org/10.1016/j.carbpol.2013.06.069.

[19] H. Zhao, N.D. Heindel, Determination of degree of substitution of formyl groups in polyaldehyde dextran by the hydroxylamine hydrochloride method, Pharm. Res. 8 (3) (1991) 400–402, https://doi.org/10.1023/A:1015866104055.

[20] B. Romberg, J.M. Metselaar, T. de Vringer, K. Motonaga, J.J. Kettenes-van den Bosch, C. Oussoren, G. Storm, W.E. Hennink, Enzymatic degradation of liposome-grafted poly(hydroxyethyl l-glutamine), Bioconjug. Chem. 16 (4) (2005) 767–774, https://doi.org/10.1021/bc0497719.

[21] Y. Gu, Y. Yang, J. Yuan, Y. Ni, J. Zhou, M. Si, K. Xia, W. Yuan, C. Xu, S. Xu, Y. Xu, G. Du, D. Zhang, W. Sun, S.Y. Zheng, J. Yang, Polysaccharide-based injectable hydrogels with fast gelation and self-strengthening mechanical kinetics for oral tissue regeneration, Biomacromolecules 24 (7) (2023) 3345–3356, https://doi.org/10.1021/acs.biomac.3c00379.

[22] W. Zhang, X. Gu, X. Liu, Z. Wang, Fabrication of Pickering emulsion based on particles combining pectin and zein: effects of pectin methylation, Carbohydr. Polym. 256 (2021), 117515, https://doi.org/10.1016/j.carbpol.2020.117515.

[23] N. Kunkit, T. Deekaikam, S. Chaimuang, J. Pekkoh, K. Manokruang, Physical hydrogels prepared from cationically modified pectin with tunable sol-gel phase transition behaviors, Int. J. Polym. Mater. Polym. Biomater. 70 (2) (2021) 131–141, https://doi.org/10.1080/00914037.2019.1695208.

[24] Z.-Q. Li, The Self-Assembly of Lanthanide Complexes Based on Acylhydrazone and Schiff Base Ligands and their Functional Properties of NIR Luminescence (in Chinese), Lanzhou University, 2018.

[25] M. Hajibeygi, S. Faramarzinia, M. Shabanian, S. Norouzbahari, J. Meier-Haack, Hydrazide-hydrazone-modified polyamide as reinforcement and dispersion aid for poly(lactic acid)/hydroxyapatite nanocomposites, Mater. Chem. Phys. 289 (2022), 126497, https://doi.org/10.1016/j.matchemphys.2022.126497.

[26] Y. Wen, Z. Xie, S. Xue, W. Li, H. Ye, W. Shi, Y. Liu, Functionalized polymethyl methacrylate-modified dialdehyde guar gum containing hydrazide groups for effective removal and enrichment of dyes, ion, and oil/water separation, J. Hazard. Mater. 426 (2022), 127799, https://doi.org/10.1016/j.jhazmat.2021.127799.

[27] J.-J. Hu, M. Wang, X.-X. Lei, Y.-L. Jiang, L. Yuan, Z.-J. Pan, D. Lu, F. Luo, J.-H. Li, H. Tan, Scarless healing of injured vocal folds using an injectable hyaluronic acid-waterborne polyurethane hybrid hydrogel to tune inflammation and collagen deposition, ACS Appl. Mater. Interfaces 14 (38) (2022) 42827–42840, https://doi.org/10.1021/acsami.2c07225.

[28] H. Winning, N. Viereck, L. Nørgaard, J. Larsen, S.B. Engelsen, Quantification of the degree of blockiness in pectins using ^{1}H NMR spectroscopy and chemometrics, Food Hydrocoll. 21 (2) (2007) 256–266, https://doi.org/10.1016/j.foodhyd.2006.03.017.

[29] C. Rosenbohm, I. Lundt, T.I.E. Christensen, N.G. Young, Chemically methylated and reduced pectins: preparation, characterisation by 1H NMR spectroscopy, enzymatic degradation, and gelling properties, Carbohydr. Res. 338 (7) (2003) 637–649, https://doi.org/10.1016/S0008-6215(02)00440-8.

[30] X. Yang, H. Yang, X. Jiang, B. Yang, K. Zhu, N.C. Lai, C. Huang, C. Chang, L. Bian, L. Zhang, Injectable chitin hydrogels with self-healing property and biodegradability as stem cell carriers, Carbohydr. Polym. 256 (2021), 117574, https://doi.org/10.1016/j.carbpol.2020.117574.

[31] M.M. Deegan, A.M. Antonio, G.A. Taggart, E.D. Bloch, Manipulating solvent and solubility in the synthesis, activation, and modification of permanently porous coordination cages, Coord. Chem. Rev. 430 (2021), 213679, https://doi.org/10.1016/j.ccr.2020.213679.

[32] J. Chen, Z. Zhai, K.J. Edgar, Recent advances in polysaccharide-based in situ forming hydrogels, Curr. Opin. Chem. Biol. 70 (2022), 102200, https://doi.org/10.1016/j.cbpa.2022.102200.

[33] H.R. Moreira, F. Munarin, R. Gentilini, L. Visai, P.L. Granja, M.C. Tanzi, P. Petrini, Injectable pectin hydrogels produced by internal gelation: pH dependence of gelling and rheological properties, Carbohydr. Polym. 103 (2014) 339–347, https://doi.org/10.1016/j.carbpol.2013.12.057.

[34] R. Yang, X. Liu, Y. Ren, W. Xue, S. Liu, P. Wang, M. Zhao, H. Xu, B. Chi, Injectable adaptive self-healing hyaluronic acid/poly (γ-glutamic acid) hydrogel for cutaneous wound healing, Acta Biomater. 127 (2021) 102–115, https://doi.org/10.1016/j.actbio.2021.03.057.

[35] J. Lou, F. Liu, C.D. Lindsay, O. Chaudhuri, S.C. Heilshorn, Y. Xia, Dynamic hyaluronan hydrogels with temporally modulated high injectability and stability using a biocompatible catalyst, Adv. Mater. 30 (22) (2018) 1705215, https://doi.org/10.1002/adma.201705215.

[36] M. Ghorbani, L. Roshangar, J.S. Rad, Development of reinforced chitosan/pectin scaffold by using the cellulose nanocrystals as nanofillers: an injectable hydrogel for tissue engineering, Eur. Polym. J. 130 (2020), 109697, https://doi.org/10.1016/j.eurpolymj.2020.109697.

[37] B. Fan, K. Zhang, Q. Liu, R. Eelkema, Self-healing injectable polymer hydrogel via dynamic thiol-alkynone double addition cross-links, ACS Macro Lett. 9 (6) (2020) 776–780, https://doi.org/10.1021/acsmacrolett.0c00241.

[38] L. Chang, R. Chang, J. Shen, Y. Wang, H. Song, X. Kang, Y. Zhao, S. Guo, J. Qin, Self-healing pectin/cellulose hydrogel loaded with limonin as TMEM16A inhibitor for lung adenocarcinoma treatment, Int. J. Biol. Macromol. 219 (2022) 754–766, https://doi.org/10.1016/j.ijbiomac.2022.08.037.

[39] Y. Lei, Y. Wang, J. Shen, Z. Cai, C. Zhao, H. Chen, X. Luo, N. Hu, W. Cui, W. Huang, Injectable hydrogel microspheres with self-renewable hydration layers alleviate osteoarthritis, Sci. Adv. 8 (5) (2022) eabl6449, https://doi.org/10.1126/sciadv.abl6449.

[40] G. Xiao, Y. Wang, H. Zhang, L. Chen, S. Fu, Facile strategy to construct a self-healing and biocompatible cellulose nanocomposite hydrogel via reversible acylhydrazone, Carbohydr. Polym. 218 (2019) 68–77, https://doi.org/10.1016/j.carbpol.2019.04.080.

[41] Y. Fu, W.J. Kao, Drug release kinetics and transport mechanisms of non-degradable and degradable polymeric delivery systems, Expert Opin. Drug Deliv. 7 (4) (2010) 429–444, https://doi.org/10.1517/17425241003602259.

[42] H. Schott, Swelling kinetics of polymers, J. Macromol. Sci. Part B 31 (1) (1992) 1–9, https://doi.org/10.1080/00222349208215453.

[43] J. Li, Z.-L. Yang, T. Ding, Y.-J. Song, H.-C. Li, D.-Q. Li, S. Chen, F. Xu, The role of surface functional groups of pectin and pectin-based materials on the adsorption of heavy metal ions and dyes, Carbohydr. Polym. 276 (2022), 118789, https://doi.org/10.1016/j.carbpol.2021.118789.

[44] B.A. Rogers, H.I. Okur, C. Yan, T. Yang, J. Heyda, P.S. Cremer, Weakly hydrated anions bind to polymers but not monomers in aqueous solutions, Nat. Chem. 14 (1) (2022) 40–45, https://doi.org/10.1038/s41557-021-00805-z.

[45] Y. Li, Q. Chen, L. Hu, Synthesis and potential application of acylhydrazone functionalized linear poly(glycidol)s, J. Mol. Liq. 367 (2022), 120458, https://doi.org/10.1016/j.molliq.2022.120458.

[46] W. Ma, X. Yang, H.-B. Liu, Z.-R. Guo, J.-L. Zhang, G.-Y. Kang, C.-Y. Yu, H. Wei, Fabrication of thermo and pH-dual sensitive hydrogels with optimized physiochemical properties via host-guest interactions and acylhydrazone dynamic bonding, React. Funct. Polym. (2023), 105513, https://doi.org/10.1016/j.reactfunctpolym.2023.105513.

[47] M. Yang, S. Zhao, C. Zhao, J. Cui, Y. Wang, X. Fang, J. Zheng, Caseinate-reinforced pectin hydrogels: efficient encapsulation, desirable release, and chemical stabilization of (−)-epigallocatechin, Int. J. Biol. Macromol. 230 (2023), 123298, https://doi.org/10.1016/j.ijbiomac.2023.123298.

[48] M.P. Paarakh, P.A. Jose, C. Setty, G. Christoper, Release kinetics–concepts and applications, Int. J. Pharm. Res. Technol. 8 (1) (2018) 12–20.

[49] C. Luo, Q. Yang, X. Lin, C. Qi, G. Li, Preparation and drug release property of tanshinone IIA loaded chitosan-montmorillonite microspheres, Int. J. Biol. Macromol. 125 (2019) 721–729, https://doi.org/10.1016/j.ijbiomac.2018.12.072.

[50] J. Kaur, V. Mehta, G. Kaur, Preparation, development and characterization of Leucaena leucocephala galactomannan (LLG) conjugated sinapic acid: a potential colon targeted prodrug, Int. J. Biol. Macromol. 178 (2021) 29–40, https://doi.org/10.1016/j.ijbiomac.2021.02.132.

[51] Z. Pourmanouchehri, S. Ebrahimi, M. Limoee, F. Jalilian, S. Janfaza, A. Vosoughi, L. Behbood, Controlled release of 5-fluorouracil to melanoma cells using a hydrogel/micelle composites based on deoxycholic acid and carboxymethyl chitosan, Int. J. Biol. Macromol. 206 (2022) 159–166, https://doi.org/10.1016/j.ijbiomac.2022.02.096.

[52] K. Sangsuriyonk, N. Paradee, A. Sirivat, Electrically controlled release of anticancer drug 5-fluorouracil from carboxymethyl cellulose hydrogels, Int. J. Biol. Macromol. 165 (2020) 865–873, https://doi.org/10.1016/j.ijbiomac.2020.09.228.